Collective excitations in soft-sphere fluids

Taras Bryk,[1,2] Federico Gorelli,[3,4] Giancarlo Ruocco,[5,6] Mario Santoro,[3,4] and Tullio Scopigno[5,6,*]

[1]*Institute for Condensed Matter Physics of the National Academy of Sciences of Ukraine, 1 Svientsitskii Street, UA-79011 Lviv, Ukraine*

[2]*Institute of Applied Mathematics and Fundamental Sciences, Lviv Polytechnic National University, 79013 Lviv, Ukraine*

[3]*Istituto Nazionale di Ottica INO-CNR, I-50019 Sesto Fiorentino, Italy*

[4]*European Laboratory for Non Linear Spectroscopy, LENS, I-50019 Sesto Fiorentino, Italy*

[5]*Dipartimento di Fisica, Universita di Roma La Sapienza, I-00185, Roma, Italy*

[6]*Center for Life Nano Science @Sapienza, Istituto Italiano di Tecnologia, 295 Viale Regina Elena, I-00161, Roma, Italy*

(Received 29 November 2013; revised manuscript received 16 September 2014; published 1 October 2014)

Despite that the thermodynamic distinction between a liquid and the corresponding gas ceases to exist at the critical point, it has been recently shown that reminiscence of gaslike and liquidlike behavior can be identified in the supercritical fluid region, encoded in the behavior of hypersonic waves dispersion. By using a combination of molecular dynamics simulations and calculations within the approach of generalized collective modes, we provide an accurate determination of the dispersion of longitudinal and transverse collective excitations in soft-sphere fluids. Specifically, we address the decreasing rigidity upon density reduction along an isothermal line, showing that the positive sound dispersion, an excess of sound velocity over the hydrodynamic limit typical for dense liquids, displays a nonmonotonic density dependence strictly correlated to that of thermal diffusivity and kinematic viscosity. This allows rationalizing recent observation parting the supercritical state based on the Widom line, i.e., the extension of the coexistence line. Remarkably, we show here that the extremals of transport properties such as thermal diffusivity and kinematic viscosity provide a robust definition for the boundary between liquidlike and gaslike regions, even in those systems without a liquid-gas binodal line. Finally, we discuss these findings in comparison with recent results for Lennard-Jones model fluid and with the notion of the "rigid-nonrigid" fluid separation lines.

DOI: 10.1103/PhysRevE.90.042301 PACS number(s): 61.20.Ja, 61.20.Lc, 62.60.+v

I. INTRODUCTION

Collective dynamics of liquids is one of the most fascinating problems of modern condensed matter physics because of the interplay of processes on different spatial and time scales [1–3] as well as because of the observed dynamic crossovers between different regions on the phase diagrams in scattering and computer simulations. From a theoretical standpoint, the only solid basis for description of collective dynamics in liquids is the hydrodynamic theory, that essentially is a collection of macroscopic fundamental conservation laws. All the theoretical descriptions of liquid dynamics or thermodynamics must be in agreement with hydrodynamic theory. In particular, the problem of propagation of collective excitations in fluids on different spatial scales must be always solved taking into account different mechanisms of sound propagation on macroscopic and nanoscales.

Time-dependent correlations, which define collective properties, can reveal hidden features of a system in distinct aggregation states. This is the case, for instance, of liquid and glass phases [4,5]. While structural properties do not really discriminate between those two states, the time correlation functions and dispersion of collective excitations show markedly different behavior. Since the dispersion of collective excitations can be measured in inelastic x-ray scattering (IXS) or inelastic neutron scattering (INS) experiments, it is a proper quantity to be associated with the dynamic features inherent to different aggregation states.

Building on a similar concept, the idea of the sensitivity of dynamic properties of fluids on the liquidlike or gaslike state of the system has been recently proposed in [6], opening the way to the understanding of the dynamic dissimilarities between low- and high-density supercritical fluids. Specifically, a purely dynamic quantity was suggested to discriminate between liquidlike and gaslike states, namely, the so-called positive dispersion of collective excitations using IXS experiments and molecular dynamics (MD) simulations on supercritical argon [7,8]. The studies revealed that the positive sound dispersion (PSD) in a dense, liquidlike supercritical fluid almost vanishes upon reducing pressure, with a cusplike behavior, on crossing an extrapolated thermodynamic line identified by the extremals of the specific heat $C_P(P)$, a thermodynamic region that could be treated as a continuation of the Widom line (maxima of the correlation length in the vicinity of the critical point) deep into the supercritical region. The Widom line does part the supercritical region of the fluid phase for a restricted range of pressures and temperatures above the critical ones into a high-density, liquidlike domain and a low-density, gaslike domain. It was then found a correlation beyond the critical point between a crossover in a dynamic observable, PSD, and thermodynamics, in terms of the Widom line. Later on, a theory of positive dispersion in supercritical fluids [9] was developed based on the approach of generalized collective modes (GCM) [10,11]. This theory was based on a thermoviscoelastic dynamic model of generalized hydrodynamics and revealed the leading role of nonhydrodynamic structural relaxation in positive sound dispersion of dense fluids. The GCM theory allowed one to obtain a condition for vanishing positive dispersion and even emergence of the negative dispersion that depends on

*Corresponding author.

the ratio between the high frequency and adiabatic speeds of sound. More detailed simulations and theoretical studies of the collective dynamics in supercritical Ar in a wide range of temperatures and densities [12] recently revealed that the dynamic line where the positive sound dispersion vanishes correlates also with the minima of the thermal diffusivity and of the kinematic shear viscosity. These findings confirmed our view of a dynamic crossover connected to thermodynamics in supercritical fluids. Furthermore, another mechanism was found for the positive sound dispersion at relatively large wave numbers taking place in the low-density region and which looks to be connected with thermal processes [12].

In the framework of finding connections between dynamic crossovers and thermodynamics, it is interesting to recall the rich debate in the literature, based on experimental results and theoretical interpretations, on a real archetypal fluid system, liquid water (see [13–20] and references therein). Indeed, in this case dynamic crossovers and a predicted Widom line, i.e., the one emanating from the predicted secondary critical point in the supercooled regime, are likely to be related. Hence, these crossovers can be used, in principle, to support the existence of such an exotic critical point, which is not accessible experimentally. Our work on connection between a dynamic crossover and thermodynamics in supercritical fluids extends part of the concepts involved in the discussion on water. This connection is verified on the long time assessed, as opposed to predicted, critical point, i.e., the point where the liquid-vapor phase transition line ends, and the corresponding Widom line, being also well assessed in an extended P-T range. Now, in order to elucidate the most fundamental aspects in the connections between the dynamic crossover, in terms of density dependence of PSD, and thermodynamics, here we consider the case of a soft-sphere fluid, which does not have interatomic attraction and gas-liquid critical point. Indeed, within the previously described scenario, one may naturally wonder about what should be expected in those systems lacking the liquid-gas binodal, such as soft-sphere model fluids. The idea that thermodynamic quantities can discriminate between "rigid" and "nonrigid" regions was challenged advancing alternative criteria based on the particles lifetime in the cage of its nearest neighbors [21,22]. A few intuitive conditions for thermodynamic and dynamic quantities were suggested in [21], which however were not related to the observed sensitivity of the positive sound dispersion [6,8] for the liquidlike or gaslike type of dynamics in fluids. In general, to date there exist mainly two points of view on the location of the dynamic crossovers in fluids: (i) the one deduced from the onset of the positive sound dispersion that takes place in correspondence of the Widom line or with the loci of minima of the thermal diffusivity and of the kinematic shear viscosity, and (ii) a crossover, that separates rigid and nonrigid fluids, which does not coincide with the Widom line and does not emanate from the critical point. All these issues revived a problem of precise calculations of dispersion of collective excitations in fluids as well as estimation of the macroscopic adiabatic speed of sound.

Furthermore, the dynamic crossover proposed in [23] builds on the idea that the zero value of the shear modulus in the entire spectrum of possible frequencies is the main feature that distinguishes the soft fluid from the rigid liquid. However, the issue of the generalized bulk and shear moduli was pretty well elaborated in the literature [2,3] and even for low-density fluids one would expect nonzero values of the high-frequency shear modulus as it was shown for the case of supercritical Ar [24].

We present here a study on soft-sphere fluids in a wide range of densities. Specifically, we determine the dispersion of longitudinal and transverse collective excitations, evaluating the behavior of the positive sound dispersion and the high-frequency shear modulus. The results clearly demonstrate that even if the maximum of C_P and the gas-liquid binodal in this system are missing, the extrema of transport properties act as a boundary between gaslike and liquidlike regions.

The remaining paper is organized as follows: In the next section, we give the details of our simulations and analysis of collective dynamics. Results on static and dynamic properties for the soft-sphere fluids are reported in Sec. III, and the Conclusions are given in the last section.

II. MOLECULAR DYNAMICS SIMULATIONS AND METHODOLOGY OF DISPERSION CALCULATIONS

Molecular dynamics simulations were performed for seven densities of a model soft-sphere fluid at $T^* \equiv T/\varepsilon = 0.5843$ using a system of 2000 particles in a cubic box subject to periodic boundary conditions. The relatively low temperature was taken because of the absence of the liquid-gas coexistence binodal on the phase diagram of soft-sphere fluids and allows us to check a possible dynamic crossover just by changing the density of fluid. The effective interaction potential for soft spheres was taken as $V_{ij}(r) = \varepsilon(\sigma/r_{ij})^{12}$ with the cutoff radius of 3.542σ. One should note that the increasing inverse power of the repulsive potential as well as a shorter than the first coordination shell cutoff radius would lead to more hard-sphere-like dynamics, while in this study we are interested mainly in the origin of dynamic crossover in fluids without attraction but with rather large cutoff radius of pretty standard repulsive potential. Henceforth, we will use reduced units $\varepsilon = \sigma = m = 1$. Note that the results in reduced quantities are universal for particular choices of potential parameters and mass of particles. All the simulations were performed in microcanonical constant energy ensemble over the production runs of 600 000 time steps with a time step $\Delta t = 0.001855$, that was well justified for our low-temperature state. The small time step for integration of equations of motion provided perfect conservation of the total energy of the system during the all production runs.

Each sixth step, we sampled the Fourier components of dynamic variables of particle density

$$n(k,t) = \frac{1}{\sqrt{N}} \sum_{i=1}^{N} e^{i\mathbf{k}\cdot\mathbf{r}_i(t)},$$

longitudinal component of mass current density

$$J^L(k,t) = \frac{m}{k\sqrt{N}} \sum_{i=1}^{N} \mathbf{k} \cdot \mathbf{v}_i(t) e^{i\mathbf{k}\cdot\mathbf{r}_i(t)},$$

and energy density

$$e(k,t) = \frac{1}{\sqrt{N}} \sum_{i=1}^{N} \varepsilon_i(t) e^{i\mathbf{k}\cdot\mathbf{r}_i(t)},$$

where $\mathbf{k}$ is the sampled wave vector, $\mathbf{r}_i$, $\mathbf{v}_i$, and ε_i are the position, velocity, and single-particle energy of the ith particle, respectively. The three collective dynamic quantities describe fluctuations of conserved quantities in monoatomic fluids and form the set of hydrodynamic variables for longitudinal dynamics. Note that the first two dynamic variables are connected by the fundamental continuity equation

$$\frac{dn(k,t)}{dt} = \frac{ik}{m} J^L(k,t).$$

In order to describe the dynamic processes beyond the hydrodynamic regime (which is observed only for very small wave numbers and long times) one has to apply generalized hydrodynamics for analysis of time-dependent correlations and sample in MD simulations nonhydrodynamic variables. Note that the nonhydrodynamic variables are chosen to be orthogonal to the hydrodynamic ones, i.e.,

$$\langle A^{\mathrm{hyd}}(-k) A^{\mathrm{nonhyd}}(k) \rangle \equiv 0,$$

that allows them to describe dynamic processes in liquids beyond the hydrodynamic regime [1,2]. Hence, the most obvious choice for the nonhydrodynamic variables is to sample the first time derivatives of the hydrodynamic ones, i.e., the first time derivatives of the longitudinal component of mass current density and of the energy density:

$$\dot{J}^L(k,t) = \frac{m}{k\sqrt{N}} \sum_{i=1}^{N} [\mathbf{k}\cdot\mathbf{a}_i(t) + i[\mathbf{k}\cdot\mathbf{v}_i(t)]^2] e^{i\mathbf{k}\cdot\mathbf{r}_i(t)},$$

$$\dot{e}(k,t) = \frac{1}{\sqrt{N}} \sum_{i=1}^{N} [\dot{\varepsilon}_i(t) + i\varepsilon_i(t)\mathbf{k}\cdot\mathbf{v}_i(t)] e^{i\mathbf{k}\mathbf{r}_i(t)},$$

where the overdot means the time derivative and $\mathbf{a}_i(t)$ is the acceleration of the ith particle. Hence, the set of dynamic variables for analysis of longitudinal dynamics in a wide range of wave numbers contained the above-mentioned five ones:

$$\mathbf{A}^{(5)}(k,t) = \{n(k,t), J^L(k,t), e(k,t), \dot{J}^L(k,t), \dot{e}(k,t)\}. \quad (1)$$

Note that the extended dynamic variables contain via the accelerations $\mathbf{a}_i(t)$ the information about instantaneous forces acting on atomic particles and therefore allow correct description of the elastic response of the system in contrast to purely hydrodynamic appoach.

The time evolution of dynamic variables simulated in MD was used for direct calculations of the time correlation functions $F_{ij}(k,t) = \langle A_i^*(k,0) A_j(k,t) \rangle$, their Laplace components $\tilde{F}_{ij}(k,z)$, and the matrix elements of generalized hydrodynamic matrix [10,11]

$$\mathbf{T}(k) = \mathbf{F}(k,t=0)\tilde{\mathbf{F}}^{-1}(k,z=0) \quad (2)$$

via the 5×5 matrices of static correlation functions $\mathbf{F}(k,t=0)$ and of Laplace-transformed time correlation functions in Markovian approximation $\tilde{\mathbf{F}}(k,z=0)$. No fit was used in calculations of the matrix elements of these matrices. The GCM methodology used in this study for calculations of dynamic eigenmodes in fluids was originally derived from the microscopic kinetic theory of extended collective modes by de Schepper and Cohen with co-workers [25] as well as from the generalized hydrodynamic theory by Kivelson and Keyes [26,27]. The microscopic theory of extended collective modes enables correct description of the hydrodynamic modes as well as of the well-defined short-wavelength collective excitations for large wave numbers [28,29]. The predictive power of the GCM approach was demonstrated on the analytic theories of nonhydrodynamic opticlike excitations in binary liquids [30,31], "fast sound" excitations in binary liquids with disparate mass [32] and charge oscillations in molten salts [33] completely supported by the MD simulations.

The thermoviscoelastic dynamic model (1) allows us to study collective processes both in hydrodynamic and elastic regimes on the same footing without neglecting (as it is usually done in simple viscoelastic analysis) thermal processes, which are very important for the dynamics of fluids. We would like to recall that on macroscopic length scales the sound in fluids (in contrast to solids) propagates adiabatically because of slow relaxation connected with diffusivity of local temperature, characterized by thermal diffusivity D_T. Namely the thermal effects in and outside the hydrodynamic region are taken into account within the thermoviscoelastic dynamic model (1), that allows consistent quantitative calculations of the dispersion of collective excitations with an account for thermal and elastic processes for large wave numbers [34].

For the transverse dynamics, the same level of treatment of nonhydrodynamic processes as in the longitudinal case is provided by the two-variable dynamic model based of the transverse component of mass current density $\mathbf{J}^T(k,t)$ and its first time derivative $\dot{\mathbf{J}}^T(k,t)$, where

$$\mathbf{J}^T(k,t) = \frac{m}{k\sqrt{2}\sqrt{N}} \sum_{i=1}^{N} [\mathbf{k}\times\mathbf{v}_i(t)] e^{i\mathbf{k}\cdot\mathbf{r}_i(t)}$$

and

$$\dot{\mathbf{J}}^T(k,t) = \frac{m}{k\sqrt{2}\sqrt{N}} \sum_{i=1}^{N} [\mathbf{k}\times\mathbf{a}_i(t) + i[\mathbf{k}\times\mathbf{v}_i(t)]\mathbf{k}\cdot\mathbf{v}_i(t)] e^{i\mathbf{k}\cdot\mathbf{r}_i(t)}.$$

The time evolution of these dynamic variables was recorded every six time steps and corresponding static and time correlation functions were calculated.

The eigenvalues and corresponding eigenvectors of the generalized hydrodynamic matrix represent the dynamic eigenmodes that can exist in the liquid on the spatial scale $\sim 2\pi/k$ for the given wave number k. The eigenvalues of $\mathbf{T}(k)$ are either real numbers $d_j(k)$ or pairs of complex-conjugated numbers $z_j(k) = \sigma_j(k) \pm i\omega_j(k)$. The former correspond to relaxing modes with the relaxation time $d_j^{-1}(k)$, while the latter to propagating modes with dispersion $\omega_j(k)$ and damping $\sigma_j(k)$. Note that the applied here GCM methodology is in the spirit of the traditional for solids eigenvalue problem for dynamic matrix, however, it is free from an assumption of local potential energy minima for atoms and additionally allows one to study relaxing modes and their effects on the dispersion of collective excitations. Analysis of the dispersion $\omega(k)$ of

acoustic modes should clarify the issue of the existence and behavior of positive dispersion in soft sphere-fluids in a very wide range of densities.

III. RESULTS AND DISCUSSION

A. Structural and thermodynamic properties

The pair distribution functions (PDF) for soft-core fluids at seven densities are shown in Fig. 1. The simulated densities covered the change in structure of the fluids from typical high-density liquid with 13 particles in the first coordination shell to practically structureless gaslike PDF. The well-pronounced first peak of PDF with an amplitude ∼2.8 for the most high-density state gets more smeared out and shows reduction of its amplitude with a decrease of the density, while the first peak of PDF shifts its location from ∼1.05 to ∼1.4. The structure factor, calculated as the instantaneous density-density correlations $S(k) = \langle n_{-k} n_k \rangle$, shows similar reduction of structural features: from well-defined first peak with an amplitude ∼2.75 and small isothermal compressibility $\kappa_T = S(k=0)/nk_BT$ at the high-density state to a practically structureless $S(k)$ for the lowest-density gaslike system (see Fig. 2). Here n and k_B are number density and Boltzmann constant, respectively. With the reduction of density, the position $k_{\max}$ of the main peak of $S(k)$ shifts from ∼7.15 to ∼4.7.

Thermodynamic quantities of interest for collective dynamics of fluids estimated in a standard way from the long-wavelength limit of generalized wave-number-dependent static correlation functions [10,25] are shown in Fig. 3. The essential advantage of the direct sampling of energy fluctuations via $e(k,t)$ and observation of their evolution in MD simulations is in a possibility to calculate the macroscopic values of the linear thermal expansion coefficient α_T, specific heats C_V and C_P, and their ratio γ. For Lennard-Jones (LJ) supercritical fluids, the dependence of specific heat at constant volume C_V on density is a monotonically increasing function, while the linear thermal expansion coefficient α_T, specific heat at constant pressure C_P, and the ratio of specific heats $\gamma = C_P/C_V$ can have maxima on different lines outcoming from the critical point (P_c,T_c). These lines merge into a single Widom line at temperatures $T < 1.1T_c$ and become practically completely smeared at $T \sim 2.5T_c$ [35]. Usually, the computer simulations nicely reproduce the density dependence of specific heats and their ratio [24] for Lennard-Jones systems simulated not close to the critical point. For soft-sphere systems the specific heat is a monotonically increasing function of density, while the linear thermal expansion coefficient and the ratio of specific heats γ are monotonically decreasing with density. γ drops down to ∼1.17 at the highest density simulated here (Fig. 3). Note that γ is a measure of coupling between the viscous and thermal processes that is important in dynamics, when the visibility of the side peaks of the dynamic structure factors is defined by the Landau-Placzek ratio of the integral intensities of the central to side peaks and which is equal to $\gamma - 1$. The smaller the Landau-Placzel ratio the more pronounced are the Brillouin peaks in dynamic structure factors $S(k,\omega)$, which correspond to propagating acoustic

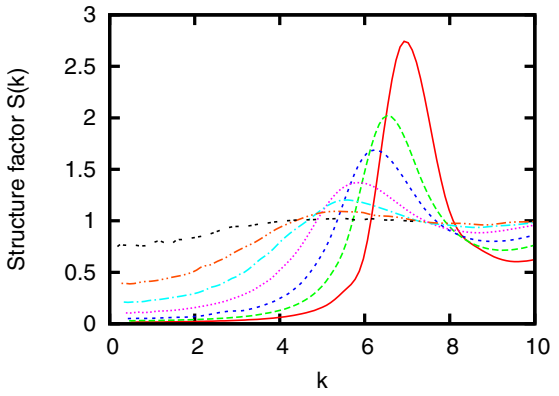

FIG. 2. (Color online) Structure factors $S(k)$ of the soft-sphere fluids for seven densities. Lines correspond to the same reduced densities as in Fig. 1.

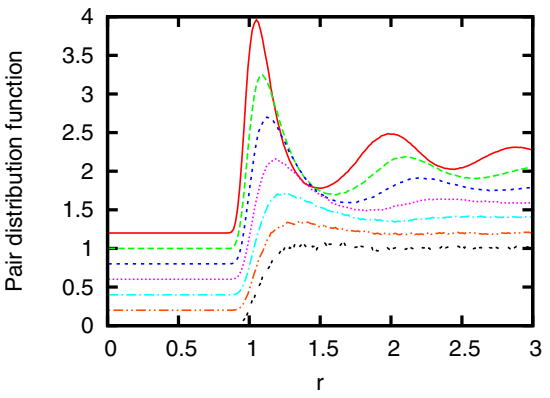

FIG. 1. (Color online) Pair distribution functions of the soft-sphere fluid for seven densities at temperature $T^* = 0.5843$. For eye convenience, a shift by 0.2 was applied to the pair distribution function by each increase of density. The lines correspond from the top to the sequence of reduced densities: 0.9648, 0.7848, 0.6352, 0.4465, 0.2976, 0.1726, and 0.0496.

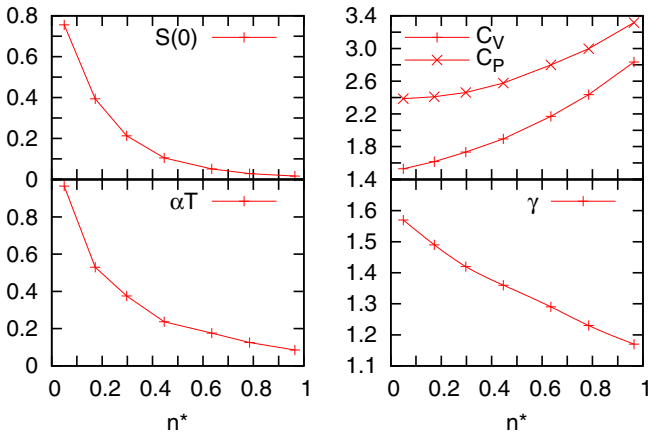

FIG. 3. (Color online) Thermodynamic quantities of the soft-sphere fluids at $T^* = 0.5843$ for seven densities: reduced isothermal compressibility $S(k=0) = \kappa_T nk_BT$, linear thermal expansion coefficient α_T, specific heats at constant volume C_V and pressure C_P in units of k_B, and ratio of specific heats γ.

modes [2]. Similarly, for heat density dynamics it was very recently shown [36] that the quantity $\gamma - 1$ is a measure of relative weights of contributions from collective excitations and heat relaxing mode to the specific heat C_V. Hence, the soft-sphere fluids at high density behave similarly to liquid metals with close to unity value of γ and $C_V \sim 3k_B$. Therefore, one can expect for the high-density soft-sphere fluids the same features of collective dynamics inherent to liquid metals.

B. Dispersion of collective excitations

The dispersions of the longitudinal (plus symbols) and transverse (cross symbols) propagating modes for soft-sphere fluids with different densities are shown in Fig. 4. One can immediately see that for high-density fluids the dispersion of longitudinal collective excitations has quite large positive dispersion in comparison with the hydrodynamic dispersion law. The values of the adiabatic speed of sound c_s as a function of density are shown in Fig. 5. The c_s was estimated from the long-wavelength extrapolation of a smooth dependence $\sqrt{\gamma(k)/S(k)}$ multiplied by the thermal velocity. To date, this is the most precise methodology of calculations of adiabatic speed of sound from classical [24] and *ab initio* [37,38] simulations. The change in the dispersion of longitudinal collective excitations with reduction of density has the following features: (i) smearing out of the well-defined maximum at $k \sim 3.5$ and minimum at $k \sim k_{\max}$. For densities smaller than $n^* = 0.2976$ the dispersion becomes a monotonically increasing function of wave number; (ii) a reduction of the positive dispersion of collective excitations with the decrease of density in the high-density region. The positive dispersion is vanishing between the densities $n^* = 0.4465$ and 0.2976, while it becomes again nonzero for further decrease of density. The last feature was observed for Lennard-Jones fluids too [9].

The theory of positive dispersion developed within the thermoviscoelastic dynamic model of generalized hydrodynamics [9] gives the first correction to the hydrodynamic dispersion law as

$$\omega_s(k) \approx c_s k + \beta k^3 + \cdots \tag{3}$$

with the prefactor β that reads as [9]

$$\beta = \frac{c_s D_L^2}{8}\frac{5 - (c_\infty/c_s)^2}{c_\infty^2 - c_s^2} - (\gamma - 1)D_T\left[\frac{6D_L + (\gamma - 5)D_T}{8c_s} - \frac{c_s}{2d_3^0}\right], \tag{4}$$

where d_3^0 is the long-wavelength limit of the kinetic thermal-stress-relaxation mode, D_L and D_T are longitudinal kinematic viscosity and thermal diffusivity, respectively, and c_∞ is the high-frequency speed of sound (6). In the case when the coupling between the thermal and viscous processes can be neglected (within a viscoelastic approximation, when the ratio of specific heats $\gamma \equiv 1$), one obtains very simple expression for the dispersion of collective excitations on the boundary of hydrodynamic regime:

$$\omega(k) \approx c_s k + \frac{c_s D_L^2}{8}\frac{5 - (c_\infty/c_s)^2}{c_\infty^2 - c_s^2}k^3. \tag{5}$$

In order to analyze the density dependence of the positive dispersion, we show in Fig. 5 the adiabatic speed of sound c_s as well as the high-frequency speed of sound c_∞ as functions of density. The latter was calculated via

$$\lim_{k\to 0}\frac{\langle \dot{J}^L(-k)\dot{J}^L(k)\rangle}{\langle J^L(-k)J^L(k)\rangle} \propto c_\infty^2 k^2. \tag{6}$$

The existence of two characteristic speeds of sound c_s and c_∞ for fluids reflects their viscoelasticity, i.e., hydrodynamic mechanism (due to conservation laws) of sound propagation on macroscopic distances and elastic mechanism on nanoscales. The high-frequency speed of sound is always higher than the adiabatic one. Figure 5 gives evidence that the high-frequency speed of sound c_∞ is well defined for all the studied densities of soft-sphere fluids. Note that c_∞ is the propagation speed in elastic medium without any account for dissipation processes and can be easily calculated either from (6) or using an integral expression for the fourth and second frequency moments of the dynamic structure factor [2], i.e., from exact sum rules. In the region of wave numbers outside the hydrodynamic region, where the elastic mechanism of sound propagation takes place, the dissipation processes, which essentially depend on k, renormalize down the c_∞ giving rise to the apparent speed of sound $c_{\rm app}(k) = \omega_{\rm sound}(k)/k$. The dissipation processes responsible for damping of acoustic collective excitations $\sigma_{\rm sound}(k)$ in the elastic regime lead to the following renormalization of the "bare" frequency [39,40]:

$$\omega_{\rm sound}(k) = \sqrt{c_\infty^2(k)k^2 - \sigma_{\rm sound}^2(k)},$$

where $c_\infty(k)$ is the wave-number-dependent high-frequency speed of sound that follows from (6). All this is in contrast with a claim made in [21] that the dynamic crossover "marks the point at which the positive dispersion disappears completely because this crossover corresponds to the complete loss of shear waves that can exist in a liquid and corresponding loss of the high-frequency sound." In fact, there is no loss of the high-frequency sound but renormalization of its propagation speed due to dissipative processes, which are usually taken into account within the memory function formalism as well as in the GCM theory.

Now, we will discuss the claimed in [21] complete "loss of shear waves" for low-density fluids. By definition [2], the generalized high-frequency shear modulus reads as follows:

$$G_\infty(k) = \frac{\rho}{k^2}\frac{\langle \dot{J}^T(-k)\dot{J}^T(k)\rangle}{\langle J^T(-k)J^T(k)\rangle} \equiv \frac{\rho}{k^2}\langle\omega^2\rangle_T(k), \tag{7}$$

where $\langle\omega^2\rangle_T$ is the normalized second frequency moment of the transverse current spectral function $C^T(k,\omega)$. In order to check the prediction of [23] that for nonrigid fluids in all the range of frequencies the shear modulus is equal to zero, that means the complete absence of shear waves in those fluids, we calculated the wave-number-dependent shear modulus $G_\infty(k)$ for different densities of our soft-sphere fluids (Fig. 6). Note that the $G_\infty(k)$ is connected with the second frequency moment $\langle\omega^2\rangle_T(k)$ of the transverse current spectral function $C^T(k,\omega)$, i.e., with the exact sum rules. The $\langle\omega^2\rangle_T(k)$ is always a positive function of wave numbers. In complete

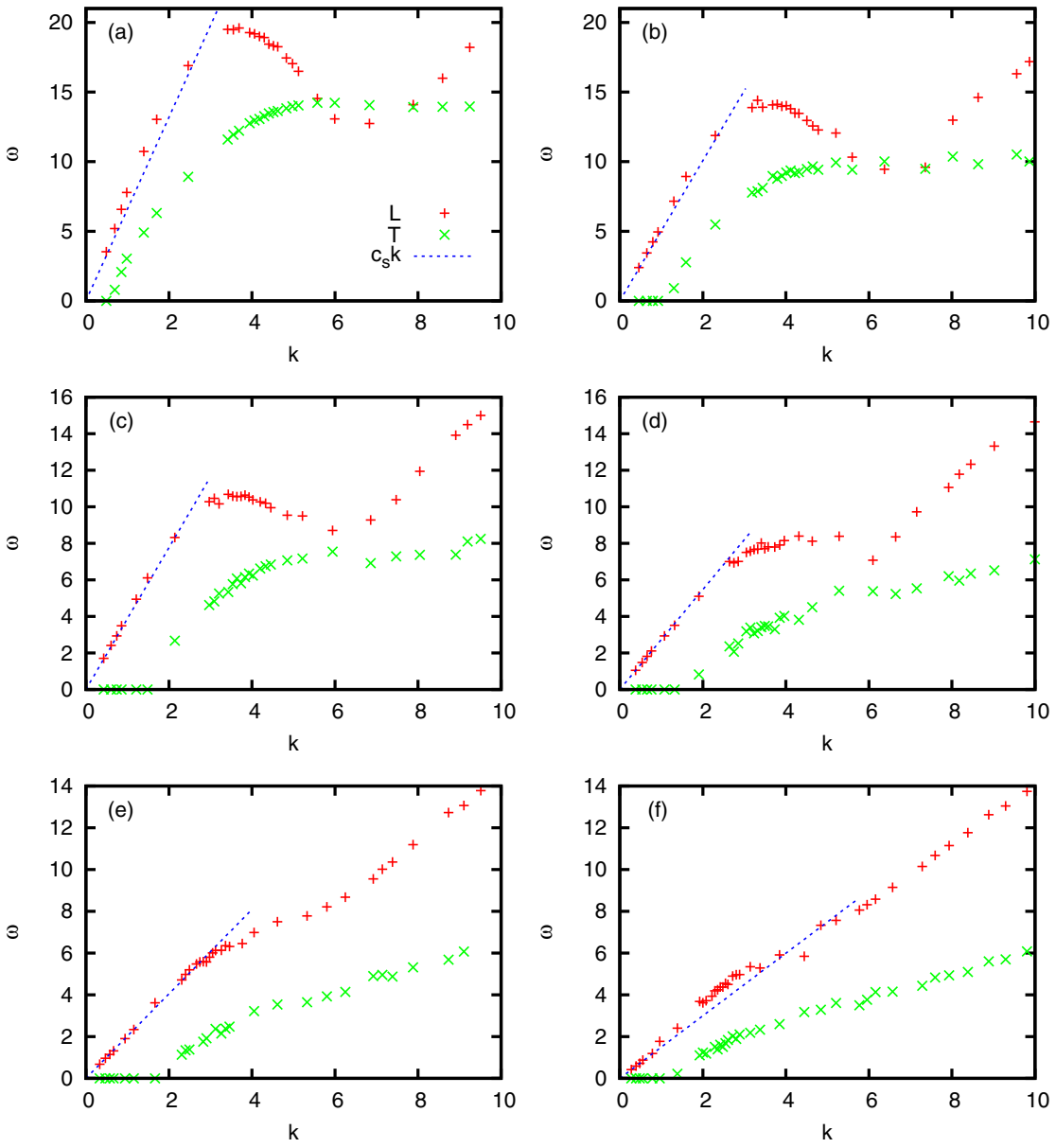

FIG. 4. (Color online) Dispersion of longitudinal (L) and transverse (T) collective excitations for soft-sphere fluids at reduced densities 0.9648 (a), 0.7848 (b), 0.6352 (c), 0.4465 (d), 0.2976 (e), and 0.1726 (f). The hydrodynamic linear dispersion law $\omega = c_s k$ is shown by a dotted line.

agreement with these arguments, we observed even for very small densities nonzero values of the high-frequency shear modulus $G_\infty(k)$. This fact completely justifies the obtained dispersion of transverse propagating eigenmodes shown by cross symbols in Fig. 4. Again, as in the case of the high-frequency sound, the dispersion of shear waves shown in Fig. 4 is the renormalized one from the frequency of "bare" shear modes, which are defined by the high-frequency shear modulus. The theory of renormalization of bare modes due to dissipative processes formulated within the perturbation theory for the generalized hydrodynamic matrix can be found in [40]. We would also like to stress that the dispersion of longitudinal collective excitations easily can be studied by finding well-defined maxima position of the longitudinal current spectral function $C^L(k,\omega)$ because of the condition $C^L(k,0) \equiv 0$. However, for the case of the transverse spectral functions $C^T(k,\omega)$ the contributions from transverse collective excitations can be hidden under the relaxing part of $C^T(k,\omega)$ because $C^T(k,0) \neq 0$. Indeed, the zero-frequency limit of the transverse spectral functions reads as $C^T(k,0) \sim \rho/[k^2\eta(k)]$, where $\eta(k)$ is the generalized shear viscosity, which tends in the long-wavelength limit to its macroscopic value η. The issue of the visibility of transverse collective excitations in $C^T(k,\omega)$ is not really well elaborated in the literature, but it is obvious that the absence of the well-defined peak in $C^T(k,\omega)$ does not mean the complete absence of shear waves propagating on nanoscales $L \sim 2\pi/k$. Similarly, the absence of a side peak in dynamic structure factors $S(k,\omega)$ for large wave numbers does not mean the lack of longitudinal collective excitations. In fact, their contribution simply is too

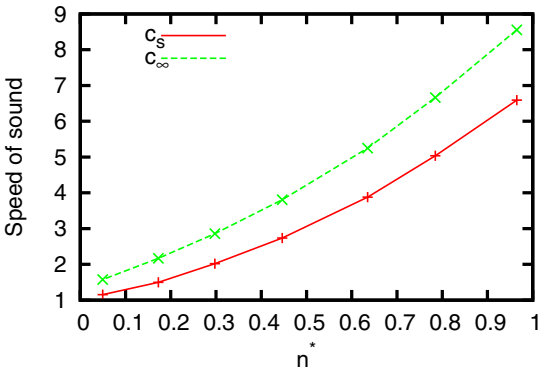

FIG. 5. (Color online) Adiabatic (line connected plus symbols) and high-frequency (line connected cross symbols) speeds of sound for the soft-sphere fluids at $T^* = 0.5843$.

weak in comparison with the one from relaxation processes. Therefore, in the case of transverse dynamics only the proper analysis based on dynamic eigenmode calculations can reveal the existence of transverse excitations, their dispersion, and contribution to $C^T(k,\omega)$ in a wide range of densities. The long-wavelength region in which the transverse collective excitations are not supported by the fluid is called a propagation gap for shear waves. For dense fluids, the reduction of the gap for shear waves with the increase of density is well known [41]. However, the sequence of dispersions for shear waves for different densities shown in Fig. 4 gives evidence that for gaslike fluids, the width of the propagation gap k_s can also decrease with reduction of density, that actually is in agreement with a theoretical prediction for the smallest wave number at which a complex-conjugated pair of transverse eigenmodes can emerge in fluids [30]

$$k_s = \frac{\sqrt{\rho G_\infty}}{2\eta}$$

taking into account the observed increase of the kinematic shear viscosity η/ρ with the decrease of density for low-density fluids [42].

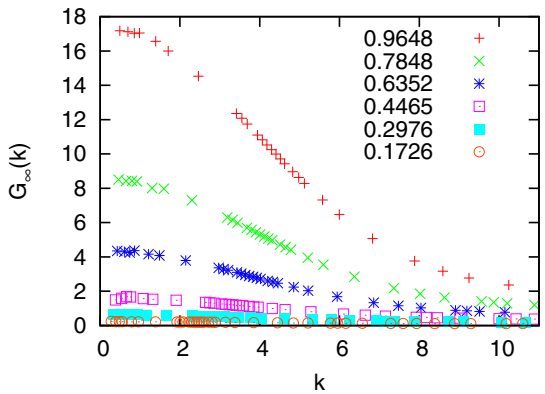

FIG. 6. (Color online) Generalized high-frequency shear modulus $G_\infty(k)$ for soft-sphere fluids at $T^* = 0.5843$ and six densities.

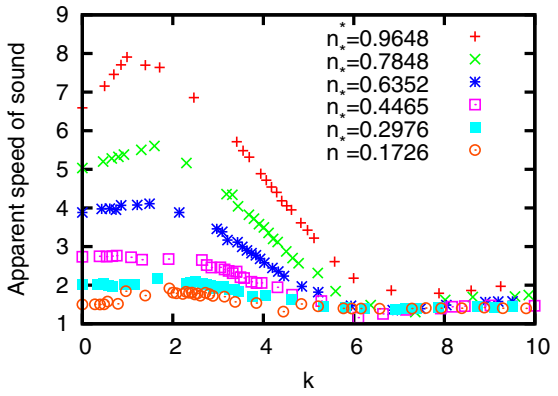

FIG. 7. (Color online) Density dependence of the apparent speed of sound $c_{app}(k) = \omega_{sound}(k)/k$ for the soft-sphere fluids at $T^* = 0.5843$ and six densities.

C. Crossover in collective dynamics of soft-sphere fluids

The crossover in collective dynamics from gaslike to liquidlike behavior was studied in [6,8,9] on the basis of positive dispersion of collective excitations in supercritical fluids. Later on, another specific nonzero positive dispersion was found in MD simulations of supercritical argon for low-density states [12]. The dispersion of collective excitations in soft-sphere fluids shown in Fig. 4 gives evidence of similar features as were observed before for supercritical fluids. In order to observe the density change of the positive dispersion, we show in Fig. 7 the apparent speed of sound $c_{app}(k) = \omega_{sound}(k)/k$. The apparent speed of sound gives evidence of a strong positive dispersion for the most dense studied here soft-sphere fluid. The positive dispersion of sound in soft-sphere fluids is reducing with the reduction of density reaching almost zero-PSD state between the densities $n^* = 0.4465$ and 0.2976 as follows from Fig. 7. For further decrease of density one observes again nonzero PSD, that gives evidence of a very similar scenario of behavior of PSD as it was observed in the case of Lennard-Jones fluids [8,12]. This means that for the systems with and without coexistence gas-liquid binodal and critical point, the behavior of the PSD is very similar.

In order to make a link between the dynamics of systems with and without the coexistence gas-liquid binodal, we calculated from the most long-wavelength dynamic eigenmodes the values of the thermal diffusivity D_T and longitudinal kinematic viscosity D_L. Their density dependence is shown in Fig. 8. Note that here, for the case of soft-sphere fluids, we observed similar $D_T(n)$ dependence as it was known for real supercritical fluids [42] and were reported in studies of critical behavior of thermal diffusivity D_T of CO_2, C_2H_6 [43], and H_2O [44]. Interestingly, both density dependencies $D_T(n)$ and $D_L(n)$ for soft-sphere fluids have minima right in the region of the smallest PSD, at the density $n^* \sim 0.37$ (see Fig. 8). Both quantities D_T and D_L define the behavior of the PSD as it follows from the analytical expression reported in Eq. (4). On the other hand, in more realistic LJ supercritical fluids (see [12]), minima in D_T and D_L have been found to correspond to maxima in C_P. When the attractive part in the Lennard-Jones potential is removed, hence in the soft-sphere potential, the Widom line is no longer defined (no gas-liquid

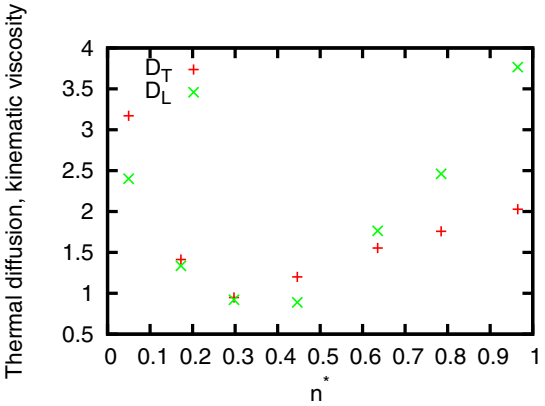

FIG. 8. (Color online) Dependence of the thermal diffusivity D_T and kinematic viscosity D_L on density for the soft-sphere fluids at $T^* = 0.5843$.

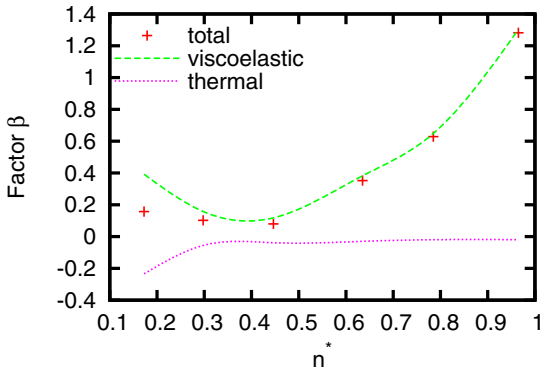

FIG. 9. (Color online) Dependence of the factor β in (4), which characterizes the leading correction to hydrodynamic dispersion law within the GCM theory. The viscoelastic and thermal contributions to β are shown by spline-interpolated dashed and dotted lines, respectively.

coexistence line and its continuation into supercritical regime) yet a link between high-frequency dynamics and macroscopic transport and thermodynamic quantities is retained. Put in different words, when soft-sphere potential is turned into the Lennard-Jones one by adding the attractive part, the correspondence between the dynamic crossover in PSD and the Widom line is reproduced. In this sense, the soft-sphere fluids support such a relationship.

For realistic fluids, the critical behavior of thermal diffusivity

$$D_T = \frac{\lambda}{nC_P}$$

depends on the divergence of thermal conductivity λ and specific heat at constant pressure C_P at the critical point [45]. The experiments [43,44] give evidence of a rapid decay of D_T on approaching the critical point, i.e., leading contribution from the C_P and, consequently, the line of the minimum of $D_T(n)$ for realistic fluids should be very close to their Widom line. This makes a strong argument in connecting the dynamic crossover in systems with and without coexistence gas-liquid binodal. We suggest here that the dynamic crossover in soft-sphere fluids takes place at the line of minima of $D_T(n)$, which almost coincides with the line of minima of $D_L(n)$. This is in agreement with our previous observations for supercritical Ar [12] as well as the very first suggestions on the role of the Widom line in the observed dynamic crossover [8]. Both quantities, thermal diffusivity and longitudinal kinematic viscosity, define the relaxation behavior of fluids because they define the hydrodynamic correlation times and damping of the long-wavelength collective excitations [1,2] as well as they define the width of hydrodynamic regime [9]. It seems that, namely, these two quantities are responsible for the dynamic crossover for all fluids: supercritical ones and soft-sphere systems. We checked out whether the GCM theory supports the correspondence between the suggested dynamic crossover with the behavior of the positive dispersion. We have calculated the density dependence of the factor β in the dispersion law of acoustic modes on the boundary of hydrodynamic regime (4). In Fig. 9, it is clearly seen that the density dependence of factor β shows a minimum with practically $\beta = 0$ right in the same region of densities where the minima of $D_T(n)$ and $D_L(n)$ are located. The leading contribution to β is of viscoelastic origin, while a nonzero negative contribution to β comes from thermal processes only in the low-density region. Hence, the GCM theory gives evidence of the nonmonotonic density dependence of the positive dispersion in soft-sphere fluids, that is completely supported by the observed apparent speed of sound $c_{\rm app}(k)$ in Fig. 7. These results that follow from the analytical GCM approach in the long-wavelength region provide the quantitative description of the crossover in PSD for soft-sphere fluids and show the factors responsible for it.

We would like to stress that the experimental studies [43,44] were performed for fluids near the critical point. Therefore, for temperatures far away from the critical region, new simulation studies for Lennard-Jones fluids are required in order to check the behavior of positive sound dispersion in a wide range of temperatures: from critical region up to very high temperatures. So far, the only study [12] was performed in this direction on supercritical Ar. Its results were in agreement with the actual findings for soft-sphere fluids on the connection of thermal diffusivity D_T and kinematic viscosity D_L with the nonmonotonic behavior of positive sound dispersion. Furthermore, the NIST database [42] allows us to follow the nonmonotonic behavior of the density dependence of D_T and D_L in very wide temperature and pressure ranges, that will definitely help in establishing their connection to the positive sound dispersion far away from the critical region in realistic liquids.

We tried also to shed light on the results on the proposed in [21] "rigid"-"nonrigid" crossover, which should be general for both supercritical and soft-sphere fluids. According to [23], "the definition of τ^* as the average time necessary for a particle to become displaced by an average interatomic distance" can be easily used to calculate τ^* from the mean square displacements $\langle R^2\rangle(t)$ and pair distribution functions for fluids of different density. Similarly, having the spectra of collective excitations, we can calculate the quantity $\tau_0 = 2\pi/\omega_{\rm max}$, where $\omega_{\rm max}$ is according to [23] "the maximum frequency of acoustic excitations (on the order of Debye frequency),"

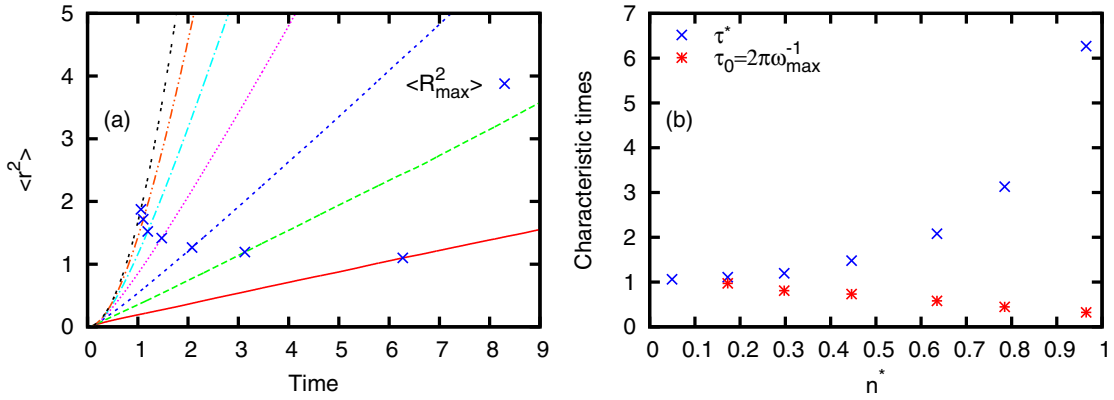

FIG. 10. (Color online) Mean square displacements (a) and calculated according to [21,23] characteristic times (b) for soft-sphere fluids at $T^* = 0.5843$. The cross symbols in (a) and (b) correspond to the $\langle R^2_{\max}\rangle$, where $R_{\max}$ are the positions of the first maximum of pair distribution function. The color and line types in (a) corresponded to the same densities as in Fig. 1.

which was estimated according to [21] from the linear sound dispersion law and "taking maximum frequency $\omega_{\max}$ as Debye frequency."

In Fig. 10, we show the behavior of the mean square displacements of the soft-sphere fluids. The time τ^* needed for particles to reach the distance $R_{\max}$, i.e., the location of the main peak of the corresponding pair distribution function, is shown by cross symbols in Fig. 10. As the $\omega_{\max}$ we took the values of observed in Fig. 4 first maxima of $\omega(k)$, which change from the well-defined one in the case of dense fluids to very smeared out in the low-density fluids, located approximately at $k_{\max}/2$, i.e., at the location of the pseudo-Brillouin zone boundary, where $k_{\max}$ is the location of the first peak of $S(k)$. For the lowest-density fluid, we did not observe a clear shoulder or maximum in dispersion in the region of $k_{\max}/2$, therefore, we did not calculate $\omega_{\max}$ for that case. From the comparison of τ^* and τ_0 in Fig. 10 one can see that the proposed in [21] criterion $\tau^* = \tau_0$ for the rigid-nonrigid crossover cannot be fulfilled. Another possibility for estimation of the τ_0 was suggested in [21] to take "the minimal period of transverse quasiharmonic waves." Looking at the dispersion of shear waves shown by cross symbols in Figs. 4(a)–4(f) one can see that it is difficult to define the maximum oscillation frequency for the shear waves. Furthermore, there is no sense to use the Debye model and to define some "Debye frequency" for shear waves because the dispersion of shear waves is not linear with k as this is for transverse modes in solids and contains the propagation gap in the long-wavelength region (see Fig. 4).

IV. CONCLUSIONS

The molecular dynamics simulations and analysis of dynamic eigenmodes, based on the GCM approach, performed on a wide range of densities of soft-sphere fluids revealed the existence of positive dispersion of collective excitations at high densities and its density evolution found to be similar to the one observed for Lennard-Jones fluids [9]. Hence, for the fluids with and without interparticle attraction, the dynamic crossover takes place in the same way. We have found that the vanishing positive dispersion corresponds to the density region where the thermal diffusivity D_T and kinematic viscosity D_L have their smallest values. These two transport quantities define the damping of long-wavelength collective excitations and main hydrodynamic correlation times. Hence, our results for soft-sphere fluids and previously for the Lennard-Jones ones allow us to conclude that the dynamic crossover between the "liquidlike" and "gaslike" states of fluids takes place with and without the gas-liquid binodal at the region where thermal diffusivity and kinematic viscosity have their minima as functions of density. As a matter of fact, in the soft-sphere fluid, i.e., the case when the Widom line is not defined, still a link between high-frequency dynamics and macroscopic transport and thermodynamics exists. On the other hand, in Lennard-Jones supercritical fluids (see [12]), minima in D_T and D_L have been found to correspond to maxima in C_P. In other words, when a soft-sphere system is turned into the Lennard-Jones one by adding the attractive part of the potential, the correspondence between the dynamic crossover in PSD and the Widom line is reproduced. In this sense, soft-sphere fluids support such a relationship. This result is clearly different from the case of supercooled liquid water, where dynamical crossovers are predicted to occur in correspondence of maxima of C_P, even in absence of the secondary critical point, i.e., when no Widom line exists [20,46].

We applied to the analysis of the PSD in soft-sphere fluids an analytical theory of the long-wavelength behavior of PSD derived in [9]. It showed similar contributions from the viscoelastic and thermal processes to PSD as was observed for supercritical Ar: at large densities, the PSD is almost completely defined by the coupling with structural relaxation, while at small densities the thermal relaxation processes connected with diffusivity of local temperature give rise to a negative contribution. For the case of supercritical fluids by approaching the Widom line and the critical point, the thermal diffusivity rapidly drops causing the large negative contribution to the PSD. Hence, the reported here combination of MD simulations, GCM analysis of eigenmodes, and analytical theory give an important quantitative description of the similarity and specific features of dynamic crossover in the systems with and without gas-liquid critical point.

Further, we discussed the dynamic crossover in fluids based on the Frenkel's idea of lifetimes of particles in the cages of nearest neighbors to the observed behavior of positive

dispersion in soft-sphere fluids [21]. Our determination of the average time τ^* for the particles to reach the first coordination shell and of the shortest period of oscillations τ_0 show that for soft-sphere fluids, these characteristic times differ and only in the very low-density limit $\tau^* \approx \tau_0$ holds. Moreover, our analysis of the density dependency of high-frequency speed of sound shows that there is no sharp loss of the rigidity of fluids. Similarly, the well-defined wave-number dependency of the high-frequency shear modulus gives evidence of the existence of the short-wavelength shear waves even in low-density soft-sphere fluids. These observations were supported by calculated transverse propagating eigenmodes, which exist in the short-wavelength region even for the lowest-density fluids, and by exact sum rules for transverse dynamics. Our results give evidence that there is no loss of shear waves for all frequencies, at variance with the idea that vanishing of shear waves is the main feature that distinguishes the soft fluid from the rigid liquid [23].

All together, our results do not support the existence of a dynamic line that separates rigid and nonrigid fluids, while positive sound dispersion behaves nonmonotonically as a function of density and can be a measure of dynamic crossovers regardless of the existence of a gas-liquid coexistence binodal on the phase diagram.

[1] J.-P. Hansen and I. R. McDonald, *Theory of Simple Liquids* (Academic, London, 1986).
[2] J.-P. Boon and S. Yip, *Molecular Hydrodynamics* (McGraw-Hill, New York, 1980).
[3] J. R. D. Copley and S. W. Lovesey, Rep. Prog. Phys. **38**, 461 (1975).
[4] W. Götze and M. R. Mayr, Phys. Rev. E **61**, 587 (2000).
[5] G. Ruocco and F. Sette, J. Phys.: Condens. Matter. **13**, 9141 (2001).
[6] F. A. Gorelli, M. Santoro, T. Scopigno, M. Krisch, and G. Ruocco, Phys. Rev. Lett. **97**, 245702 (2006).
[7] F. A. Gorelli, M. Santoro, T. Scopigno, M. Krisch, T. Bryk, G. Ruocco, and R. Ballerini, Appl. Phys. Lett. **94**, 074102 (2009).
[8] G. Simeoni, T. Bryk, F. A. Gorelli, M. Krisch, G. Ruocco, M. Santoro, and T. Scopigno, Nat. Phys. **6**, 503 (2010).
[9] T. Bryk, I. Mryglod, T. Scopigno, G. Ruocco, F. Gorelli, and M. Santoro, J. Chem. Phys. **133**, 024502 (2010).
[10] I. M. Mryglod, I. P. Omelyan, and M. V. Tokarchuk, Mol. Phys. **84**, 235 (1995).
[11] T. Bryk, I. Mryglod, and G. Kahl, Phys. Rev. E **56**, 2903 (1997).
[12] F. A. Gorelli, T. Bryk, M. Krisch, G. Ruocco, M. Santoro, and T. Scopigno, Sci. Rep. **3**, 1203 (2013).
[13] L. Xu, P. Kumar, S. V. Buldyrev, S.-H. Chen, P. H. Poole, F. Sciortino, and H. E. Stanley, Proc. Natl. Acad. Sci. USA **102**, 16558 (2005).
[14] P. Kumar, S. V. Buldyrev, S. R. Becker, P. H. Poole, F. W. Starr, and H. E. Stanley, Proc. Natl. Acad. Sci. USA **104**, 9575 (2007).
[15] L. Xu, F. Mallamace, Z. Yan, F. W. Starr, S. V. Buldyrev, and H. E. Stanley, Nat. Phys. **5**, 565 (2009).
[16] G. Franzese and H. E. Stanley, J. Phys.: Condens. Matter **19**, 205126 (2007).
[17] K. Chakraborty and S. Bandyopadhyay, J. Phys. Chem. B **118**, 413 (2013).
[18] S. Pawlus, S. Khodadadi, and A. P. Sokolov, Phys. Rev. Lett. **100**, 108103 (2008).
[19] S.-H. Chen, L. Liu, X. Chu, Y. Zhang, E. Fratini, P. Baglioni, A. Faraone, and E. Mamontov, J. Chem. Phys. **125**, 171103 (2006).
[20] M. G. Mazza, K. Stokely, S. E. Pagnotta, F. Bruni, H. E. Stanley, and G. Franzese, Proc. Natl. Acad. Sci. USA **108**, 19873 (2011).
[21] V. V. Brazhkin, Yu. D. Fomin, A. G. Lyapin, V. N. Ryzhov, and K. Trachenko, Phys. Rev. E **85**, 031203 (2012).
[22] V. V. Brazhkin, Yu. D. Fomin, A. G. Lyapin, V. N. Ryzhov, E. N. Tsiok, and K. Trachenko, Phys. Rev. Lett. **111**, 145901 (2013).
[23] V. V. Brazhkin, A. G. Lyapin, V. N. Ryzhov, K. Trachenko, Yu. Fomin, and E. Tsiok, Phys. Usp. **55**, 1061 (2012).
[24] T. Bryk and G. Ruocco, Mol. Phys. **109**, 2929 (2011).
[25] I. M. deSchepper, E. G. D. Cohen, C. Bruin, J. C. van Rijs, W. Montfrooij, and L. A. de Graaf, Phys. Rev. A **38**, 271 (1988).
[26] T. Keyes and D. Kivelson, J. Chem. Phys. **54**, 1786 (1971).
[27] D. Kivelson and T. Keyes, J. Chem. Phys. **57**, 4599 (1972).
[28] I. M. deSchepper and E. G. D. Cohen, J. Stat. Phys. **27**, 223 (1982).
[29] I. M. deSchepper, P. Verkerk, A. A. van Well, and L. A. de Graaf, Phys. Rev. Lett. **50**, 974 (1983).
[30] T. Bryk and I. Mryglod, J. Phys.: Condens. Matter **12**, 6063 (2000).
[31] T. Bryk and I. Mryglod, J. Phys.: Condens. Matter **14**, L445 (2002).
[32] T. Bryk and I. Mryglod, J. Phys.: Condens. Matter **17**, 413 (2005).
[33] T. Bryk and I. Mryglod, J. Phys.: Condens. Matter **16**, L463 (2004).
[34] A. Z. Akcasu and E. Daniel, Phys. Rev. A **2**, 962 (1970).
[35] V. V. Brazhkin, Yu. D. Fomin, A. G. Lyapin, V. N. Ryzhov, and E. N. Tsiok, J. Phys. Chem. B **115**, 14112 (2011).
[36] T. Bryk, G. Ruocco, and T. Scopigno, J. Chem. Phys. **138**, 034502 (2013).
[37] L. Calderin, L. E. Gonzalez, and D. J. Gonzalez, J. Phys.: Condens. Matter **25**, 065102 (2013).
[38] T. Bryk and G. Ruocco, Mol. Phys. **111**, 3457 (2013).
[39] L. D. Landau and E. M. Lifshitz, *Mechanics* (Butterworth-Heinemann, Oxford, 2005).
[40] T. Bryk and I. Mryglod, Condens. Matter Phys. **11**, 139 (2008).
[41] T. Bryk and I. Mryglod, Phys. Rev. E **62**, 2188 (2000).
[42] E. W. Lemmon, M. O. McLinden, and D. G. Friend, in *NIST Chemistry WebBook, NIST Standard Reference Database Number 69*, edited by P. J. Linstrom and W. G. Mallard (National Institute of Standards and Technology, Gaithersburg, MD, 2009), http://webbook.nist.gov
[43] D. E. Wetzler, P. F. Aramendia, M. L. Japas, and R. Fernandez-Prini, Int. J. Thermophys. **19**, 27 (1998).
[44] J. V. Sengers, R. A. Perkins, M. L. Huber, and B. Le Neindre, Int. J. Thermophys. **30**, 1453 (2009).
[45] P. Jany and J. Straub, Int. J. Thermophys. **8**, 165 (1987).
[46] P. Kumar, G. Franzese, and H. E. Stanley, Phys. Rev. Lett. **100**, 105701 (2008).